

Restoring the Lifespan of Road Pavement in Durham Region in Ontario, Canada, through Innovative Quality Assurance Testing of Recovered Asphalt Binder

Dariusz Kokabi
Master's Student
Queen's University
Kingston, Ontario
Dariusz.Kokabi@queensu.ca

Jianmin Ma
Postdoctoral Research Fellow
Queen's University
Kingston, Ontario
Jianmin.Ma@queensu.ca

Hanwalle M.C. Nawarathna
Research Associate
Queen's University
Kingston, Ontario
cpn1@queensu.ca

Simon A.M. Hesp
Professor
Queen's University
Kingston, Ontario
Simon.Hesp@queensu.ca

Paper prepared for the session SO - Testing, Modelling and Innovation for Roadway/Embankment
Materials and Geotechnical Engineering
2024 Transportation Association of Canada (TAC) Conference & Exhibition
Vancouver, British Columbia

Acknowledgements

Funding for this research was generously provided by The Regional Municipality of Durham, the Bitumen Beyond Combustion program of Alberta Innovates (Agreement Numbers 212201460 and 232404554), the Discovery Grant program of the Natural Sciences and Engineering Research Council of Canada (Grant Numbers RGPIN-2018-03730 and RGPIN-2024-04161). Past contributions to this research program by numerous students and funding agencies over many years are hereby also gratefully acknowledged. The pavement condition assessments were provided by an independent, third-party consultant for the Regional Municipality of Durham and can be made available upon reasonable request. The consultant was unaware of the change in specification in 2015 and the authors only received his reports in 2023. Finally, staff from Durham Region are thanked for their help in collecting HMA samples for this study.

Abstract

One of the best ways to manage the performance lifespan of asphalt road surfaces is to test recovered binder for acceptance during construction. In the late 1990s, acceptance specifications advanced from using empirical methods, such as penetration and viscosity on unaged binder in the Canadian General Standards Board (CGSB) specification of 1990 to Superpave™ rheology-based tests on unaged and laboratory-aged residue. In the early 2000s, Ontario agencies realized that poor-quality binder was responsible for premature and excessive cracking of road surfaces, after which enhanced aging, rheological and failure tests for unaged and recovered material were developed and implemented. This study correlates pavement service lives in Durham Region with recovered binder properties. Service lives to a pavement condition index (PCI) of 50 percent – which had decreased by about 66 percent since 1980 – bounced back immediately after the 2015 implementation of the double-edge-notched tension (DENT, AASHTO T 405) and extended bending beam rheometer (EBBR, AASHTO T 406) protocols for the acceptance of recovered binder. Both protocols favor the use of superior quality Alberta and Venezuela binders that are low in wax and contain a moderate amount of asphaltenes. Today, proper designs based on EBBR grade and grade loss in conjunction with DENT critical crack tip opening displacement (CTOD) have restored pavement service lives from 11 years in 2013 to their former 30-35 years in 2020.

1. Introduction

Canada has a vast road network. The total length of public roads is estimated at 1.13 million kilometers, of which approximately 40 percent is paved.¹ Over 90 percent of paved roads are made from asphalt because it has advantages over the alternative, which is Portland cement concrete (PCC). Asphalt roads have become an indispensable part of our transportation infrastructure as they contribute enormously to the safe and effective operation and development of socio-economic activities in Canada and beyond.

Binder durability has been a research topic of interest for many decades.²⁻⁷ Durability is determined by the consistency of properties and resistance to distresses such as rutting, aggregate polishing, cracking, raveling, potholes and so forth, encountered during a pavement's service life as a result of environmental conditions and repeated traffic loading.⁸ In this regard, the primary objective of asphalt pavement design is to enhance its resilience against various types of distress throughout its service life, ensuring the pavement achieves its maximum benefit/cost performance.^{9, 10} The asphalt pavement design process involves material and structural design.¹¹ Material design focuses on properly selecting raw materials, such as asphalt binder,^{12, 13, 14-16, 17} aggregates and fillers.^{18, 19} Structural design involves determining the optimal arrangement of pavement layers as well as their gradation type and thickness.²⁰ Normally, the structural design of asphalt pavements in a given region undergoes minimal changes after being established through long-term practice.²¹ However, variations in the source of raw materials can lead to significant differences in asphalt pavement quality. Asphalt mixture can simply be regarded as a two-phase system: aggregates form the structural skeleton, while asphalt mastic fills the pore space and binds the aggregates together.²² Given that asphalt binder exhibits time-temperature-dependent viscoelastic behavior, it imparts flexibility to the pavement, and accounts for the resistance to permanent deformation at elevated temperatures and cracking due to repeated traffic and low-temperature shrinkage.^{23, 24} Therefore, the properties of the binder are crucial for determining pavement durability. Considering this, tremendous efforts have been devoted to developing and implementing effective, practical performance acceptance tests of asphalt binder.²⁵⁻²⁸

Over the decades, numerous test methods have been developed to select optimal asphalt binders for pavement construction and rehabilitation. The penetration grading system, standardized by the American

Association of State Highway and Transportation Officials (AASHTO) in 1931, was designed to categorize asphalt for application in different climates.²⁹ The penetration test is an empirical method measuring how deep a standard needle penetrates an asphalt sample at 25°C under a specified load and duration. The detailed procedure was embodied in one of the earliest American Society for Testing and Materials (ASTM) standards.³⁰ Penetration specification protocols typically specify minimum and maximum penetration values for materials to be accepted into contracts. It is noteworthy that the penetration test is based on empirical methods and does not quantify binder consistency in strictly scientific measurements. However, for straight binders, it does have the advantage of relating strongly to the viscous component of deformation. Then again, evaluating binder behavior at 25°C – a temperature close to the average during asphalt pavement service – might not accurately reflect its performance under temperatures that are significantly lower or higher.^{3, 31} Hence, another empirical indicator, penetration index (PI), was developed as a supplement to evaluate temperature susceptibility. Early research found that asphalt binders identical in penetration but with differences in PI can exhibit extraordinary differences in cracking resistance.^{3, 32}

Another grading system is the viscosity method, which provides the handling characteristics for the asphalt binder as well as a measure of the amount of paraffin oils present. Binder viscosity can be determined using a rotational viscometer at 135°C and a capillary tube viscometer at 60°C. These two values were chosen to replicate the temperatures of the asphalt mixture during the mixing and transportation processes as well as during compaction in the field, respectively. The methodologies for measuring asphalt viscosity at 60°C and 135°C are detailed in ASTM D2170³³ and ASTM D4402³⁴ standard specifications, respectively.

The Canadian Government Standards Board specification CAN/CGSB-16.3-M90 Asphalt Cement for Road Purposes provided a measure of binder quality in terms of temperature susceptibility.³⁵ The CGSB specification classified materials in three performance groups: A (good), B (medium) and C (poor). CGSB specifications required the measurement of penetration at 25°C and absolute viscosity at 60°C. Kinematic viscosity at 135°C could be used instead of absolute viscosity at 60°C in a slightly modified format of the specification.³⁵ The benefit of the CGSB specification arose from the fact that it provided an indirect measure of durability through the strong dependence of penetration and viscosity on binder constitution (in particular, asphaltene and paraffin content), and thus ability to flow over the temperature range typically encountered in service. However, it was recognized early on that the specification was less appropriate for modified binders.

The Superpave performance grading (PG) system represents the most widespread approach for the grading and specifying of asphalt binders in North American road construction. Initiated in 1987, the Strategic Highway Research Program (SHRP) was funded by the United States Department of Transportation, leading to the development of the Superpave specification. This specification is officially recognized by AASHTO.³⁶ Different from the penetration and viscosity grading systems that measure physical properties at constant temperatures to estimate the overall properties of asphalt binder, PG specification methods measure fundamental properties of asphalt binders at temperatures corresponding to those experienced by pavements, focusing on addressing critical distress forms such as permanent deformation (rutting), fatigue cracking, and thermal or low-temperature cracking.³⁷ For example, PG 64-22 indicates the binder grades in the PG system and should be able to withstand a seven-day average high temperature of 64°C and a once in 50-years low temperature of -22°C. The intermediate- and low-temperature performance grades of asphalt are assessed using a dynamic shear rheometer (DSR) and bending beam rheometer (BBR), respectively, with asphalt samples subjected to short-term and long-term aging, representing the most severe conditions under which cracks are prone to develop in asphalt

pavements.³⁸ While the Superpave PG system has brought substantial improvements, its limitations are becoming increasingly apparent with the rapid proliferation in the use of polymer modified asphalt, reclaimed asphalt pavement (RAP) and diluent oils such as re-refined engine-oil bottoms (REOB), which were not thoroughly considered during the 5-year SHRP effort.^{14-16, 39-48}

In response to these challenges, new performance acceptance testing methods have been developed to characterize performance-related properties accurately. Considering that the durability of most Canadian asphalt pavements is predominantly influenced by the cracking resistance of the asphalt binder, the discussion hereinafter will focus exclusively on related test methods. The cracking types here refer to thermal and fatigue cracking, according to their causes. It was found that asphalt pavement fatigue originates and spreads within the asphalt binder itself. However, the parameter $|G^*| \cdot \sin \delta$, which is based on the concept of dissipated energy and measured within the linear viscoelastic range at small strains, may not fully capture the actual damage.⁴⁹⁻⁵¹ Later research revealed a weak correlation between $|G^*| \cdot \sin \delta$ and indicators of mixture fatigue, underscoring the necessity to address binder-related damage in specifications.⁴⁹⁻⁵¹ Alternative fatigue-cracking resistance tests include the time sweep test, binder yield energy test, and linear amplitude sweep test.^{40, 52, 53} The primary distinction between these lies in the application of higher stress or strain amplitudes and an increased number of loading cycles.

Apart from fatigue cracking, thermal stress induced transverse cracking is the most common distress form in asphalt pavement, especially in cold regions. Thermal cracking occurs when the thermal stress exceeds the tensile strength of asphalt binder. However, this was not fully considered in the current BBR protocol. Alternative new methods, such as double-edge-notched tension (DENT) test,⁵⁴⁻⁵⁶ asphalt binder cracking device (ABCD),⁵⁷ and single-edge-notched bending (SENB) test^{25, 58} have been proposed. Among these, the DENT is the most successful in ranking binders with different resistance to fatigue.⁵⁹ The method, first published as draft standard LS-299 by the Ministry of Transportation of Ontario (MTO) in 2005, has been utilized to accept large volumes of Ontario asphalt cement since 2010.^{60, 61} It was adopted as a provisional AASHTO standard in 2015,^{7, 53, 62-65} and obtained full status under AASHTO designation T 405 in 2023.⁶⁶

Over the decades, the DENT test protocol has undergone extensive validations, including round-robin and correlation analysis, which marks a significant effort to mitigate cracking in cold climates.^{14-16, 43, 50, 51, 56, 59} The main criterion obtained is the critical crack tip opening displacement (CTOD), a key measure of strain tolerance for an asphalt binder in the ductile state and under severe constraint.^{50, 51, 67} The development and implementation of the DENT test represents a proactive approach to improving pavement durability by addressing the challenges of ductile failure and enhancing the fatigue life of the road surface.

It has long been recognized that asphalt binders gradually change in consistency when left to equilibrate at or below room temperature.^{4, 5, 13, 68-76} To address these observations in a binder acceptance framework, the extended bending beam rheometer (EBBR) test was developed⁷⁷ and extensively validated with prematurely failed contracts and road test sections.^{12-17, 78-80} The EBBR protocol rewards superior quality binders manufactured from Alberta and Venezuelan crude sources as they are low in wax, contain a moderate amount of asphaltenes and are therefore highly durable.^{10, 12-14, 81} First published as Ministry of Transportation of Ontario laboratory standard LS-308,⁷⁷ first adopted for evaluating asphalt cement in Kingston, Ontario,⁶⁴ and later more broadly across the province,⁶¹ the test provides a critical assessment tool for measuring thermo-reversible aging tendencies in asphalt binders as this is not considered in the regular BBR method.^{7, 17, 64, 65, 82-85} Informed by the seminal research of Traxler and colleagues^{70-72, 86} as well as additional explorations into thermo-reversible aging that mainly resulted from isothermal crystallization or phase separation,^{5, 68, 69, 73} the EBBR method was developed to quantify changes in the hardness and relaxation ability of asphalt binder due to isothermal conditioning at low temperatures. This

method was later embodied in AASHTO provisional standard TP 122,⁸⁷ and obtained full status under designation T 406 in 2023.⁸⁸ It has been implemented for acceptance of asphalt binder in numerous Ontario paving contracts since 2010.⁶¹

Results from pavement trials and regular contracts have shown that the durability of Ontario's asphalt pavements can be extended to a satisfactory level by implementing the two advanced binder performance testing protocols.^{10, 14-16, 64, 65} The objective of this study was to assess the effectiveness of AASHTO T 405 DENT and AASHTO T 406 EBBR protocols for acceptance testing of recovered asphalt binder in road construction contracts in the Regional Municipality of Durham. The service lives of 968 road segments over 2,400 lane kilometers dating back to the late 1970s were assessed to provide an overview of the evolution of average lifespan over recent decades and to reveal how changes in binder specification have affected sustainability. The specification test results for the recovered asphalt binders from a subset of these road segments were correlated with the corresponding projected service life data to validate our working hypothesis that advanced binder acceptance methods can extend service lives for asphalt pavements in cold climates. Recommendations for addressing challenges associated with the reduced service lives of asphalt pavements, potentially caused by introducing new additives and modifiers, are proposed to refine methods or propose practical alternatives.

2. Materials and Methodology

2.1. Materials

In this study, a total of 41 hot mix asphalt (HMA) samples were obtained through Durham Region's quality assurance sampling program during the construction phase of new asphalt pavements between 2015 and 2021. Subsequently, these samples underwent careful extraction and recovery processes and accelerated pressure aging vessel (PAV) aging to produce residue for further testing. All binders were tested according to AASHTO T 405 DENT and AASHTO T 406 EBBR standard protocols. Additional binders were tested but not included in this study as precise location information was unavailable. Other binders have since been recovered and tested but these are also omitted from this analysis as early pavement condition data cannot be used to project pavement service life with sufficient confidence.

2.2. Methods

2.2.1 Extraction and Recovery

Asphalt mixture samples from the road segments described earlier were processed through a careful extraction and recovery procedure at Queen's University to produce asphalt binder for further aging and testing. This process, depicted in Figure 1, encompasses the following steps: (i) First, the asphalt mixture is immersed in dichloromethylene (DCM) solvent overnight to ensure the complete dissolution of the asphalt binder; (ii) Second, the sample is sieved to remove coarse and fine aggregates. Aggregates are washed with fresh DCM to remove remaining asphalt; (iii) Third, the asphalt solution is fed through a high-speed centrifuge to remove most of the fines; (iv) Fourth, the solution is transferred into a round bottom flask which is heated in an oil bath at temperatures increasing from 90°C to 160°C, while rotating under an applied vacuum maintained at 550 mbar initially and slowly reduced to below 50 mbar. This process, which takes approximately 2 hours, is conducted under a dry nitrogen gas atmosphere to prevent the aging of the binder. After evaporating most of the solvent, the temperature is gradually increased in steps to ensure the complete recovery of the pure binder; (v) Then, the recovered binder is aged using the PAV according to standard procedures.⁸⁹ The aging conditions involve exposing the asphalt film of 3.2 mm

thickness to 100°C for 20 hours under a compressed air pressure of 2.10 MPa. Following the PAV aging process, the PAV-aged residue is subjected to performance evaluation tests, including the DENT and EBBR tests.

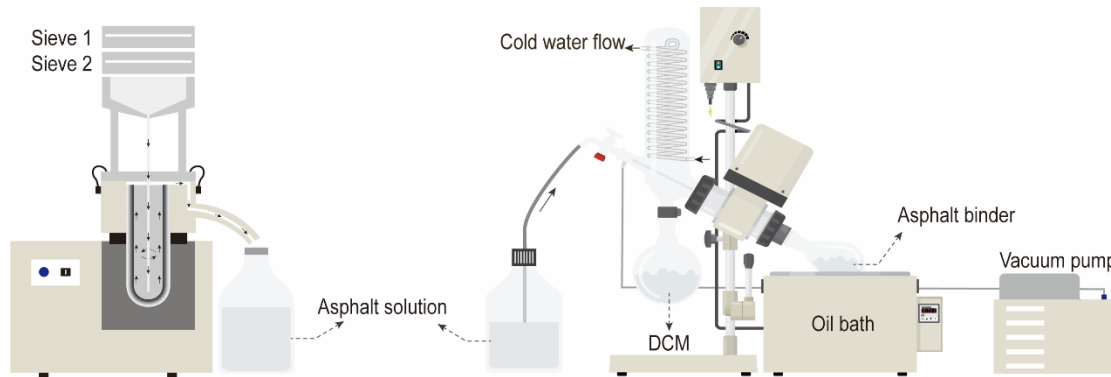


Figure 1. Schematic diagram of the extraction and recovery process of asphalt binder from mix.

2.2.2 AASHTO T 405 DENT

The AASHTO T 405 DENT test was conducted according to standard protocols.⁶⁶ In the test, six specimens with three notch depths (ligament lengths of 5 mm, 10 mm and 15 mm) were prepared for each binder. Each notch depth was tested in duplicates. Samples were subjected to tensile testing at a controlled rate of 50 ± 2.5 mm/min inside a 15°C water bath until failure. A typical force-displacement curve is shown in Figure 2. The fracture energy determined, based on the area under the force-displacement curve, was used to calculate the specific total work of failure W_t as shown in Eq. (1). The W_t is defined as the sum of the total essential work of failure, W_e , and the total plastic work, W_p , as expressed in Eq. (2). Eq. (2) can be rewritten by assuming that the essential work is proportional to the cross-sectional area of the ligament (calculated as specimen thickness multiplied by ligament length), and the plastic work corresponds to a volume around the ligament, as depicted in Eq. (3):

$$W_t = \int_0^{t_f} P \times d \quad (1)$$

$$W_t = W_e + W_p \quad (2)$$

$$W_t = L \times B \times w_e + \beta \times L^2 \times B \times w_p \quad (3)$$

Where W_t is the specific total work of fracture, MPa; W_e is the total essential work of fracture, J; W_p is the plastic fracture work, J; w_e is the specific essential fracture work, kJ/m²; βw_p is the specific plastic fracture work term, MJ/m³; t_f is the time to reach ductile fracture, s; P is the tensile force, N; d is the displacement, mm; L is the width of the ligament, mm; B is the height of the ligament, mm.

After obtaining the force-displacement curve shown in Figure 2(c), the total specific fracture work W_t is fitted with the ligament length L to obtain w_e and βw_p . The intercept and slope of the fitting line represent the essential fracture work w_e and the plastic work term βw_p , respectively. Therefore, the total specific fracture work w_t can be calculated using Eq. (4). The CTOD value was determined using data from the specimen with the smallest ligament width (5 mm), as per Eqs. (5) and (6):

$$w_t = \frac{W_t}{L \times B} = w_e + \beta w_p \times L \quad (4)$$

$$\sigma_{n=5mm} = \frac{P_{peak}}{B \times L} \quad (5)$$

$$CTOD_{L=5mm} = \frac{w_e}{\sigma_{L=5mm}} \quad (6)$$

Where σ represents the net section stress, N/mm²; P_{peak} represents the average maximum load, N; L represents the ligament length, mm; B represents the thickness of the ligament, mm.

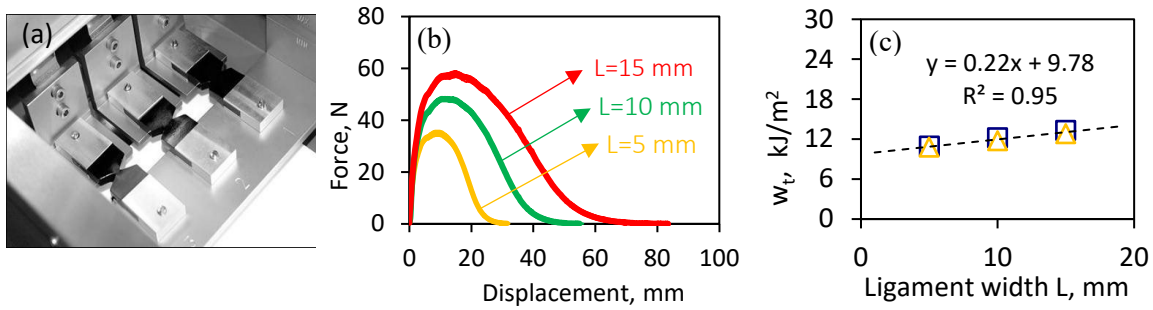


Figure 2. Schematic of the AASHTO T 405 DENT test: (a) Asphalt samples in water bath; (b) Representative load-displacement curves for DENT samples with different ligament lengths, L; (c) Determination of essential failure and plastic works from intercept and slope, respectively. Duplicate measurements provide representative repeatability.

2.2.3 AASHTO T 406 EBBR

AASHTO T 406 EBBR tests were performed using the standard protocol.^{14, 88} Twelve beams as shown in Figure 3 (b) were subjected to conditioning in ethanol baths maintained at temperatures of $T_d + 10$ and $T_d + 20$, where T_d represents the designated low temperature for the pavement design as determined by the LTPPBind™ software. Each bath accommodated six beams for conditioning. Three beams from each bath were tested at intervals following 1 h, 24 h, and 72 h of conditioning. After conditioning, the asphalt beam is positioned on the two support points. A vertical force of 980 ± 50 mN was applied to the center of the beam and maintained for 240 s. The deflection versus time curve is shown in Figure 3(b). After the test, the creep stiffness $S(t)$ was calculated according to Eq. (7):

$$S(t) = \frac{PL^3}{4bh^3\Delta(t)} \quad (7)$$

Where $S(t)$ is the creep stiffness at time t, MPa; P is the vertical load, mN; L is the distance between the two supporting points at the bottom of the asphalt small beam, 102 mm; B and h represent the width and thickness of the beam, which are 12.5 mm and 6.25 mm, respectively; $\Delta(t)$ The mid span deflection of the asphalt beam at time t, mm.

The creep stiffness $S(t)$ at 60 s is determined and the corresponding tangent slope or m value at that point in logarithmic coordinates is also determined. Among them, $S(t)$ reflects the hardness of the binder while

the m value represents the creep rate, both of which are closely related to cracking resistance at low temperatures. After obtaining $S(t)$ and m values at two temperatures, the continuous grading temperatures based on the two indicators, namely, $T_{C,s}$ and $T_{C,m}$, are calculated where the $S(t) = 300$ MPa and m value = 0.3, respectively, according to Eqs. (8) and (9):

$$T_{C,s} = T_i + \left[\frac{(T_i - T_{i+1}) \cdot (\log(300) - \log(S_i))}{\log(S_i) - \log(S_{i+1})} \right] \quad (8)$$

$$T_{C,m} = T_i + \left[\frac{(T_i - T_{i+1}) \cdot (0.3 - m_i)}{(m_i - m_{i+1})} \right] \quad (9)$$

Where T_i is the i -th test temperature, °C; S_i is the stiffness at the i -th temperature, MPa; m_i is the m value at the i -th temperature. The grade loss for the continuous grade after 72 hours of conditioning is finally determined to evaluate the thermo-reversible aging tendency and durability of the asphalt binder.

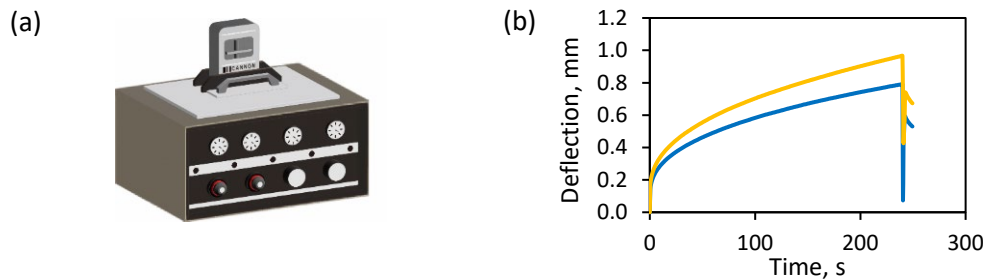


Figure 3. (a) BBR equipment; (b) typical deflection curves after 1 h (gold) and 72 h (blue) conditioning.

2.2.4 Field Survey of Distresses

Pavement condition evaluation is critical to pavement management to ensure roads remain functional. It facilitates implementation of necessary rehabilitation measures to extend service life. Pavement condition index (PCI) is a quantitative measure of the overall road condition. It consists of two major components: ride comfort rating (RCR) and the distress manifestation index (DMI). RCR represents the functional performance of the road, such as roughness; and is assigned a value between 0 and 10 to indicate the ride quality. In contrast, the DMI reflects the structural integrity; and quantifies the degree of pavement distress. These two components should be obtained by considering the total length of road section that has a single pavement condition. Given that RCR assesses driving ease, comfort and safety, factors compromising the RCR include excessive or uneven crowning, wash boarding, raveling and bumpiness resulting from issues, such as cracking, sealing and uneven patching. These inadequacies are critical when evaluating the overall quality of the driving experience. This assessment can be conducted subjectively or with mechanical devices. In this study, both methods were employed to obtain the PCI. All PCI data were obtained by a retired government engineer with about 40 years of experience in rating pavement conditions. The individual was unaware of the change in specifications in 2015, and the authors only obtained his complete data set in early 2023. Hence, human bias was not a factor in any of the analysis presented herein. For DMI, distresses were classified into 27 categories, and a detailed guideline was provided to determine the severity of each type of distress.^{90,91} In this study, DMI was calculated as per Eq. (10):

$$DMI = \sum_{i=1}^n w_i (s_i + d_i) \quad (10)$$

Where w_i is the weighting value for each distress; s_i and d_i are the severity and the density of distresses, respectively, both on a scale from 0 to 4. The PCI can be calculated through Eq. (11):

$$PCI = \sqrt{100 \cdot (0.1 \cdot RCR)} \cdot \frac{(205 - DMI)}{205} \times c + s \quad (11)$$

Where c and s are calibration constants. If RCR is calculated by automated methods, then c is 1.077 and s is 0. If RCR is determined subjectively, c and s are 0.924 and 8.856, respectively.⁹⁰ The primary methodology employed by Durham Region for reporting the PCI involves two key components: structural adequacy and surface condition. Structural adequacy represents distress manifestations and is scored between 0 and 20, while the surface condition, corresponding to the RCR, ranges from 0 to 10. These components are evaluated by an experienced consultant. PCI calculation involves multiplying structural adequacy by surface condition, followed by division by 2 to yield a PCI score out of 100.

Ontario municipalities use different evaluation strategies, such as the Inventory Manual, overall condition index, pavement quality index, structural adequacy index, and PCI. However, for paved roads, municipalities are now required to report an average PCI value at regular intervals.⁹² While the RCR and structural adequacy can be measured precisely by using automated or mechanical methods, the most common procedure is a visual inspection of the road. Video imaging or scan-type methods have been developed to survey distresses, but they are not widely accepted as they are prone to pick up artifacts.

In the current study, the results of yearly field surveys for distresses in different road segments were sourced from the Durham Region Infrastructure for Roads Report. This report provides a comprehensive overview of each road section, including the PCI, length, and year of construction or major rehabilitation. The dataset encompasses 968 road sections, cumulatively spanning about 2,400 lane kilometers. In addition to PCI assessments, data on the average annual daily traffic (AADT) was also extracted. The AADT estimates the average daily traffic volume for a particular road segment over the span of one year, and was categorized into four levels, as outlined in Table 1 for 576 segments with available AADT data.

Table 1. Number of road segments and length in each AADT category.

| AADT | Segments | Total length, km |
|-------------|----------|------------------|
| < 5000 | 129 | 85 |
| 5000-10000 | 140 | 80 |
| 10000-20000 | 171 | 68 |
| > 20000 | 136 | 32 |

3. Results and Discussion

3.1. Service Life Improvements from Enhanced Acceptance Specifications

In this study, PCI results for 968 road segments dating as far back as 1976 were included. For pavements constructed in the same year, that thus have the same age, the mean PCI was calculated, and the findings are shown in Table 2. The lifespan of each road section was determined by either the realized service life (i.e., the point at which PCI reached 20 percent and 50 percent) or the projected one, using PCI data from 2018 to 2023. The service lives for road segments constructed were obtained by linear fitting of the average PCI versus age data and forcing the lines through 100 percent at age zero as shown in Figure 4(a) for a select number of ages. The findings for all segments are shown in Figure 4(b).

The average results are shown in Figure 4(b), which shows a substantial 66 percent reduction in average pavement service life over just 28 years, dropping from 33 years in 1986 (average of 4 segments) to just 11 years by 2013 (average of 29 segments). This agrees with the 50-60 percent decrease in the average service life for provincial roads in Ontario over 25 years, as reported by the Office of the Auditor General of Ontario in 2016.⁶¹ With the progressive application of modifiers and recycled asphalt, the Superpave performance acceptance tests, as implemented in the late 1990s, appear to have had no beneficial effect on improving asphalt durability. Asphalt contaminated with harmful modifiers or additives such as REOB, RAP or recycled asphalt shingle (RAS) can easily pass the Superpave acceptance tests, and this has had negative consequences for network sustainability.^{7, 14-16, 43, 64, 93, 94} This contrasts with data after 2015 when the improved specifications were implemented.

Table 2. Mean PCI values for all road segments constructed or rehabilitated (1976-2021).

| Last Construction | Age, years | Segments | Mean Pavement Condition Index (PCI), % | | | | |
|-------------------|------------|----------|--|------|------|------|------|
| | | | 2018 | 2019 | 2020 | 2021 | 2023 |
| 1976 | 48 | 1 | 18 | 18 | 18 | 15 | 15 |
| 1979 | 45 | 7 | 32 | 40 | 40 | 29 | 26 |
| 1981 | 43 | 1 | 42 | 42 | 39 | 38 | 32 |
| 1983 | 41 | 4 | 18 | 18 | 18 | 18 | 19 |
| 1984 | 40 | 3 | 29 | 28 | 24 | 25 | 21 |
| 1986 | 38 | 4 | 48 | 48 | 45 | 43 | 42 |
| 1987 | 37 | 19 | 24 | 23 | 22 | 22 | 22 |
| 1988 | 36 | 5 | 42 | 37 | 36 | 33 | 26 |
| 1989 | 35 | 9 | 45 | 45 | 38 | 38 | 37 |
| 1990 | 34 | 28 | 22 | 21 | 17 | 17 | 16 |
| 1991 | 33 | 19 | 31 | 31 | 28 | 28 | 24 |
| 1992 | 32 | 10 | 50 | 47 | 46 | 45 | 37 |
| 1993 | 31 | 24 | 27 | 28 | 27 | 26 | 25 |
| 1994 | 30 | 60 | 37 | 35 | 32 | 31 | 29 |
| 1995 | 29 | 11 | 53 | 51 | 50 | 45 | 45 |
| 1996 | 28 | 27 | 43 | 42 | 39 | 39 | 35 |
| 1997 | 27 | 36 | 45 | 42 | 37 | 36 | 35 |
| 1998 | 26 | 19 | 50 | 50 | 45 | 46 | 41 |
| 1999 | 25 | 15 | 38 | 35 | 31 | 29 | 27 |
| 2000 | 24 | 13 | 53 | 42 | 41 | 36 | 32 |
| 2001 | 23 | 28 | 54 | 51 | 45 | 43 | 37 |
| 2002 | 22 | 38 | 54 | 49 | 43 | 42 | 36 |
| 2003 | 21 | 21 | 63 | 59 | 54 | 47 | 44 |
| 2004 | 20 | 15 | 51 | 44 | 40 | 37 | 32 |
| 2005 | 19 | 19 | 50 | 45 | 41 | 39 | 34 |
| 2006 | 18 | 33 | 56 | 48 | 46 | 40 | 37 |
| 2007 | 17 | 14 | 57 | 55 | 47 | 38 | 34 |
| 2008 | 16 | 32 | 70 | 65 | 60 | 55 | 50 |
| 2009 | 15 | 60 | 68 | 65 | 58 | 55 | 50 |
| 2010 | 14 | 53 | 67 | 62 | 57 | 52 | 51 |
| 2011 | 13 | 22 | 69 | 68 | 65 | 63 | 58 |
| 2013 | 11 | 29 | 69 | 65 | 63 | 58 | 56 |
| 2014 | 10 | 9 | 93 | 90 | 85 | 72 | 69 |
| 2015 | 9 | 43 | 90 | 90 | 87 | 85 | 80 |
| 2016 | 8 | 51 | 88 | 89 | 85 | 84 | 83 |
| 2017 | 7 | 22 | 91 | 90 | 86 | 84 | 82 |
| 2018 | 6 | 22 | 87 | 91 | 89 | 88 | 84 |
| 2019 | 5 | 42 | --- | 94 | 96 | 92 | 89 |
| 2020 | 4 | 36 | --- | --- | 97 | 96 | 95 |

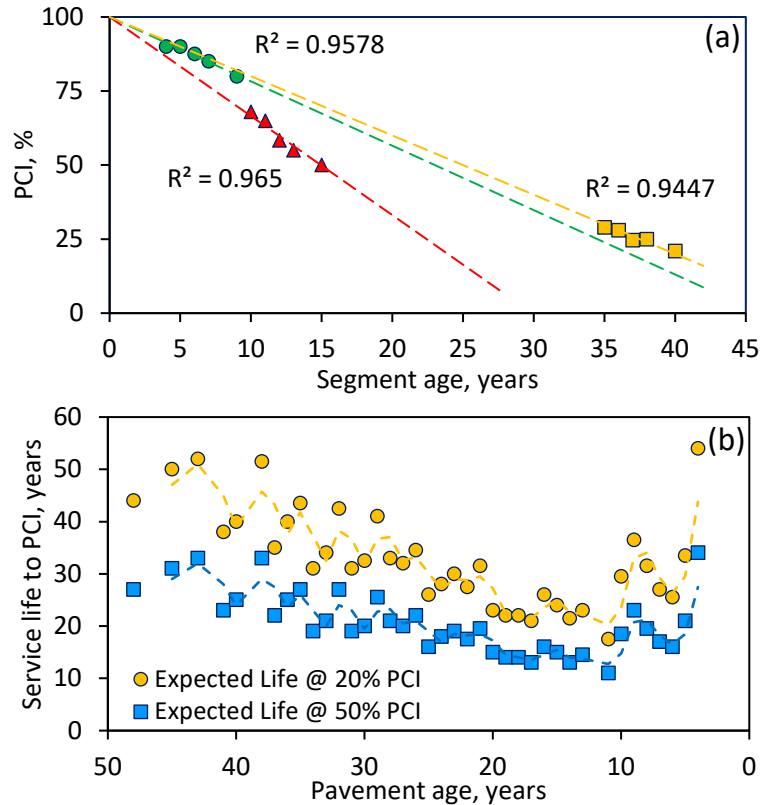


Figure 4. Historical service lives for 968 Durham Region road segments. (a) Extrapolations to realized and projected average service lives (gold squares for 1984 (3 locations, 40 years old, realized average life = 25 years), red triangles for 2009 (43 locations, 15 years old, realized average life = 15 years), green circles for 2015 (47 locations, 9 years old, projected average life = 23 years), (b) Average service lives versus age for 968 road segments (trendlines are moving averages with a period of two, gold circles for 20 percent PCI limit, blue squares for 50 percent PCI limit, 1984 (25 years), 2013 (11 years) and 2020 (34 years)).

3.2. Effect of Traffic on Deterioration Rate

Traffic volume plays a crucial role in influencing the durability of asphalt pavement. With the availability of AADT data for many road segments, the following discussion examines the impact of traffic volume on the PCI deterioration rate. To facilitate this analysis, the AADT ratings were categorized into four groups. PCI data corresponding to each group are presented in Figure 5. To better understand the effect of the specification changes, the PCI data within each group have been separated into two subgroups: before and after the implementation of the enhanced specifications in 2015. Figure 5 shows the difference in the obvious deterioration rates of pavement condition before and after 2015 for lower traffic volumes (AADT < 20,000, improvements of 25, 25 and 35 percent for 5(a), 5(b) and 5(c), respectively). One reason for why there is no significant improvement for high-volume roads (AADT > 20,000, improvement of 2 percent for 5(d)) might be that the enhanced testing methods only fail binders that are prone to thermal cracking, but they are less useful to control rutting distress. In the case of high-traffic volumes, rutting may be the dominant cause of deterioration of the pavement PCI. This issue deserves further investigation as the realized service lives for these roads are suboptimal at around 16-17 years.

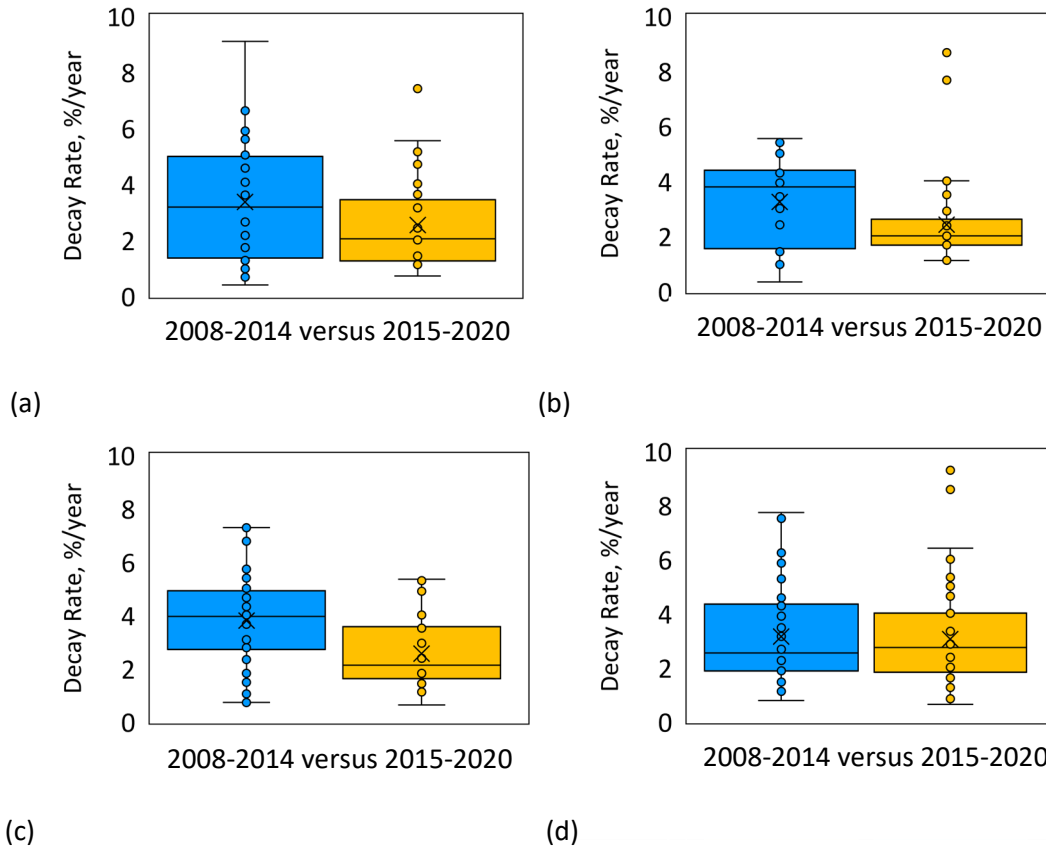


Figure 5. Box and whisker plots of PCI decay rates versus pavement age for different traffic levels (377 road segments, selected data points overlap in the graphs): (a) AADT \leq 5,000 (38 for 2008-2014 and 42 segments for 2015-2020); (b) 5,000 < AADT \leq 10,000 (34 for 2008-2014 and 39 segments for 2015-2020); (c) 10,000 < AADT \leq 20,000 (81 for 2008-2014 and 38 segments for 2015-2020); (d) AADT > 20,000 (47 for 2008-2014 and 58 segments for 2015-2020). Note that results for 2012 were not available.

3.3. Effect of Binder Properties on Deterioration Rates

In this section, the latest PCI deterioration rates obtained from the 2023 Durham Region Infrastructure for Roads Reports for segments constructed and rehabilitated from 2015 to 2020, representing pavements constructed under the enhanced specifications, were compared with data from 2002 to 2014, associated with roads built according to Superpave.³⁶ To clarify trends as well as variability in the data, box and whisker plots were constructed as shown in Figure 6. The box encompasses 50 percent of the data (i.e., the interquartile range), the horizontal lines within each box provide the median decay rates in PCI, the crosses within each box provide the average decay rates in PCI, and the entire data set for each period and traffic level is given between the whisker bounds. Outliers are defined as points that lie beyond 1.5 times the interquartile range away from the upper and lower limits for each box. Both data within and outside the box are given as symbols for each construction year. The change in PCI deterioration rate with pavement age for asphalt pavements constructed before versus after 2015 demonstrated a significant change for the better. The average rate for blue is 3.4 percent/year while for gold it is 2.0 percent/year, a 41 percent improvement over the timeframe indicated.

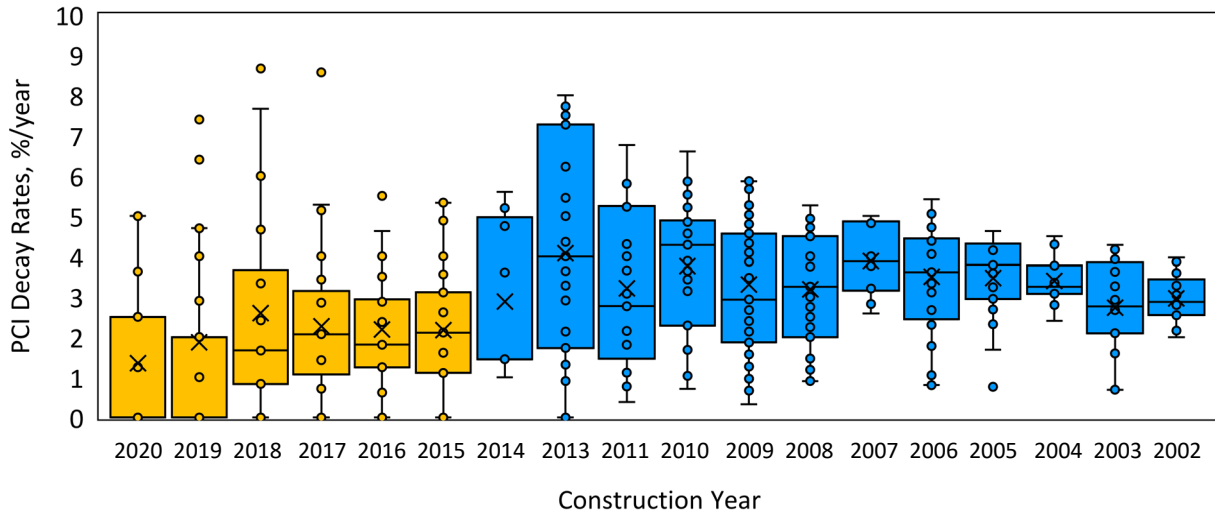


Figure 6. Box and whisker plot for PCI decay rates versus pavement age for pavement segments constructed before (blue) and after (gold) 2015 (538 data points, results for 2012 were not available, selected data points overlap in the graph).

3.4. Effect of Recovered Binder Properties on PCI Deterioration Rates

Based on the above analysis, it can be concluded that the durability of asphalt pavement can be substantially enhanced by adopting enhanced binder testing methods. These improved testing protocols can identify asphalt binders that may detrimentally impact durability – a level of discrimination not attainable with conventional binder testing approaches that are uncoupled from performance. To further substantiate this conclusion, EBBR and DENT test data obtained previously for asphalt binders from different pavement sections with known field performance were compared with PCI decay rates. The grade loss as an estimation of thermo-reversible aging was determined through AASHTO T 406 EBBR testing while the CTOD was calculated from the AASHTO T 405 DENT test. Our previous studies on trial sections and prematurely failed contracts have shown that low-temperature cracking resistance of asphalt binder can be improved by limiting grade loss and increasing the CTOD.^{7, 10, 64}

A threshold grade loss of 3°C was established to categorize the road sections into two groups. The 3°C limit was highly discriminating for a series of eastern Ontario paving contracts with extraordinary variability in performance.¹⁶ Analysis was then applied separately to these two datasets as shown in Figure 7(a). Additionally, an EBBR limiting low-temperature PG grade (LLTPG) threshold of -28°C was employed to divide the PCI data into two additional groups, facilitating linear fitting to predict the lifespan of asphalt roads constructed with binders exhibiting diverse low-temperature EBBR grades, as shown in Figure 7(b). A limit on the DENT CTOD of 14 mm was used to assess the effect of ductile strain tolerance on pavement durability, the results of which are shown in Figure 7(c).

It can be deduced from Figure 7 that road pavement built with binders characterized by better EBBR and DENT performance exhibit greatly extended service lives. In contrast, the current AASHTO standard R 320 is unlikely to differentiate binders with different cracking resistance.¹⁶ The AASHTO R 320 standard employs a fatigue factor to evaluate the fatigue-cracking resistance of asphalt binders. For thermal-cracking resistance, creep stiffness and stress relaxation rate were used to evaluate different asphalt binders. It is obvious that AASHTO R 320 overlooks thermo-reversible aging performance and high-strain

failure characteristics of asphalt binders. Extensive validation efforts have demonstrated that these two properties are crucial in determining the overall cracking resistance of asphalt pavements.^{7, 14, 16, 17, 43, 59, 64, 65, 82-85} The findings presented in Figure 7 further confirm that the field performance of pavements can be enhanced significantly by controlling the degree of thermo-reversible aging, gelation and ultimately the failure resistance of the binder. This conclusion is in broad agreement with the work of McLeod³² and our own work on pavement trials and prematurely cracked contracts.^{14-16, 17, 43, 64}

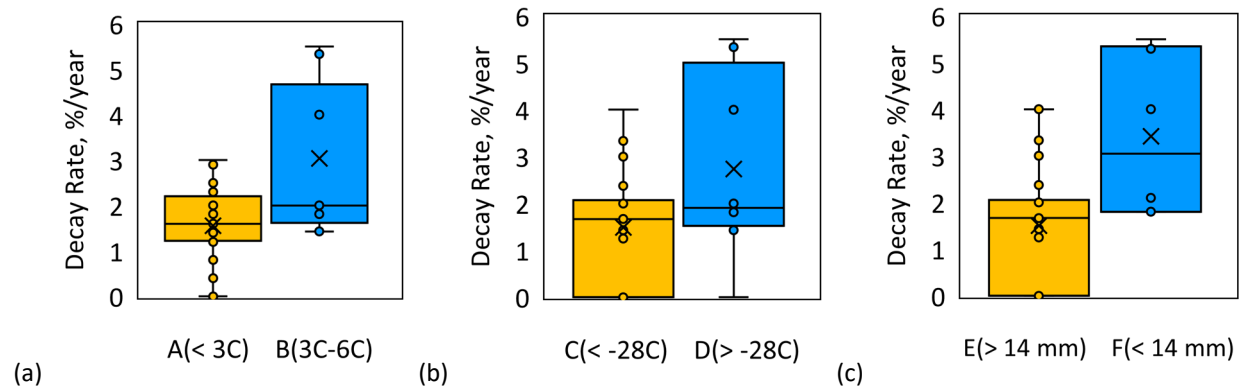


Figure 7. Box and whisker plots for PCI decay rates of road segments classified according to EBBR and DENT results for extracted and recovered binder (41 segments constructed since 2015). (A) Grade loss < 3°C (29 segments), (B) Grade loss > 3°C and < 6°C (9 segments), (C) LLTPG < -28°C (31 segments), (D) LLTPG > -28°C (8 segments), (E) CTOD > 14 mm (35 segments), and (F) CTOD < 14 mm (6 segments).

4. Summary and Conclusions

This study performed a comprehensive analysis of PCI data for 968 asphalt road segments in Durham, Ontario, Canada, dating back to the 1970s. The average service life for these roads was assessed to show how asphalt acceptance criteria affect durability and ultimately sustainability. Further, a correlation analysis for service lives with DENT and EBBR results was used to validate the effectiveness of the innovative acceptance criteria implemented in 2015. Observations and conclusions are as follows:

(1) The average service life of asphalt pavements in Ontario has fallen dramatically since the 1980s, despite the implementation of Superpave specifications and the use of increased levels of polymer modifiers. This decline can partially be attributed to incomplete and therefore inaccurate Superpave specifications that fail to address the well-documented thermo-reversible aging effect in asphalt binders, which has introduced a gradually increasing bias error in the acceptance specifications. The increased use of RAP and possibly incompatible oils in the HMA supply chain is likely to explain why pavements are under-designed by ever-increasing amounts.

(2) Traffic volume significantly influences the deterioration rate for ride quality and pavement condition index. Lower traffic volume roads (AADT < 20,000) have shown noticeable improvements in performance after 2015 due to the implementation of enhanced acceptance criteria. However, at higher traffic volumes, fatigue cracking due to structural design insufficiencies and rutting might predominate, reducing the effectiveness of the enhanced binder testing methods. This issue deserves further investigation as the 16-17-year service lives currently obtained for major arterial roads in Durham Region is suboptimal.¹⁰ Other reasons for why there was little change in the high traffic roads might be because the premium asphalt mixes used for these do not allow any RAP, were overdesigned with too much polymer modifier and/or were not compacted sufficiently to prevent premature aging.

(3) The adoption of advanced performance acceptance specifications after 2015, specifically EBBR and DENT test methods, led to a marked improvement in pavement durability. Analysis shows a 41 percent increase in the average service life of pavements constructed between 2015 and 2020 compared to those built between 2002 and 2014, highlighting the critical role of these testing methods in extending pavement life. Service lives have increased by as much as threefold between 2013 and 2020.

(4) The intrinsic performance-based properties of asphalt binders, as determined by EBBR and DENT tests, significantly affect field performance. Asphalt binders with lower grade loss and higher CTOD values contribute to extended pavement durability. The findings emphasize the necessity of applying enhanced binder testing protocols to identify and mitigate potential durability issues, suggesting that current standards may be inadequate for differentiating asphalt binder performance effectively.

5. Outlook

Although the DENT and EBBR tests have proven to be highly successful, there remains room for improvement. Alternative tests are being developed that may replace the DENT and EBBR. The characteristic of these new methods is their ability to assess the same key properties as DENT and EBBR with a far smaller sample size, reduced testing time, and less procedural complexity.

Preliminary studies have already indicated a strong correlation between the limiting phase angle temperature and the results obtained from DENT and EBBR tests.⁸⁴ This means that one could rely solely on DSR to arrive at a practical and accurate asphalt binder acceptance test. However, switching directly from EBBR to DSR methodology probably overlooks oil exudation effects – since ethanol in the BBR conditioning bath may remove some oil from the asphalt binder – and this cannot be achieved in an accelerated DSR protocol.^{48,97} To address this, a simple, precise, and efficient test method was developed to remove the incompatible paraffinic oil fraction prior to determining the limiting phase angle temperatures in the DSR instrument.⁴⁸ This approach is being further validated through laboratory experiments and field data analysis.

Bans on the presence of deleterious additives, as recently included in Ontario Provincial Standard Specification 1101 (OPSS.MUNI 1101), will also need to be enforced, as binders sold in Ontario continue to be tainted with considerable amounts of REOB. REOB and, similarly, other saturated oils can suffer from premature oxidative and thermo-reversible hardening as well as exudative hardening.^{48, 93, 94}

The reduced service life findings for Ontario pavements suggest that the way in which RAP is used in HMA needs to be revisited. Pavements can be recycled in more sustainable ways, such as through hot in-place recycling (HIR) since it has a track record.⁹⁵ Using only the coarse fraction of the RAP, and thereby reducing the replaced binder content, in combination with superior quality, soft Alberta binder might provide a more sustainable way forward. However, it is advisable that test sections be constructed first to investigate whether this would be an environmentally and economically sound practice.

Finally, there is a significant marketing effort by several suppliers to sell highly modified binders containing 6-8 percent of styrene-butadiene polymer with performance grade spans that are as much as 20-25°C beyond what is specified in the contract documents. While such binders can pass all binder acceptance tests with ease, their performance in service for regular HMA designs has been disappointing.¹⁰ Hence, they should be controlled through limits on the grade span and/or the slope of the phase angle master curve.^{10, 96}

References

1. Swarna S.T., Hossain K., Bernier A., 2022. Climate change adaptation strategies for Canadian asphalt pavements; Part 2: Life cycle assessment and life cycle cost analysis. *J. Clean. Prod.*, 370, 133355.
2. Lytton R., 2000. Characterizing asphalt pavements for performance. *J. Transp. Res. Board*, 1723, 5–16.
3. Pfeiffer J.Ph., Van Doormaal P.M., 1936. The rheological properties of asphaltic bitumen. *Journal of the Institute of Petroleum Technologists*, 22(37), 414–440.
4. Blokker P.C., Van Hoorn H., 1959. Durability of bitumen in theory and practice. *Proc., Fifth World Petroleum Congress, Section VI, Paper 27, June 1-5*, 417–432.
5. Struik L.C.E., 1978. *Physical Aging in Amorphous Polymers and Other Materials*, Elsevier Scientific.
6. Gooswilligen G. Van, De Bats F.Th., Harrison T., 1989. Quality of paving grade bitumen: A practical approach in terms of functional tests, *Proc., 4th Eurobitume Symposium*.
7. Angius E., Ding H., Hesp S.A.M., 2018. Durability of asphalt binder. *Constr. Build. Mater.* 165, 264–271.
8. Peraka N.S.P., Biligiri K.P., Kalidindi S.N., 2021. Development of a multi-distress detection system for asphalt pavements: Transfer learning-based approach. *J. Transp. Res. Board*, 2675(10), 538–553.
9. Blab R., 2013. Performance-based asphalt mix and pavement design. *Rom. J. Transp. Infrastr.*, 2, 21–38.
10. Ma J., Hesp S.A.M, Chan S., Li J.Z., Lee S., 2022. Lessons learned from 60 years of pavement trials in continental climate regions of Canada. *J. Chem. Eng.*, 444, 136389.
11. Lavin P., 2003. *Asphalt pavements: A practical guide to design*. CRC Press.
12. Zhao M.O., Hesp S.A.M., 2006. Performance grading of the Lamont, Alberta C-SHRP pavement trial binders. *Int. J. Pav. Eng.*, 7 (3), 199–211.
13. Hesp S., Iliuta S., Shirokoff J., 2007. Reversible aging in asphalt binders. *Energy Fuels*, 21, 1112–1121.
14. Hesp S.A.M., Genin S.N., Scafe D., Shurvell H.F., Subramani S., 2009. Five-year performance review of a northern Ontario pavement trial: validation of Ontario's Double-Edge-Notched Tension (DENT) and Extended Bending Beam Rheometer (BBR) test methods. *Proc., Can. Tech. Asphalt Assoc.*, 54, 99–126.
15. Hesp S.A.M., Kodrat I., Scafe D., Soleimani A., Subramani S., Whitelaw L., 2009. Rheological testing of asphalt cements recovered from an Ontario pavement trial. *Proceedings, Sixth International Conference on Maintenance and Rehabilitation of Pavements and Technological Control, Torino, Italy*, 84–93.
16. Hesp S., Soleimani A., Subramani S., Phillips T., Smith D., Marks P., Tam K., 2009. Asphalt pavement cracking: Analysis of extraordinary life cycle variability in Ontario. *Int. J. Pavement Eng.*, 10(3), 209–227.
17. Rigg A., Duff A., Nie Y., Somuah M., Tetteh N., Hesp S.A.M, 2017. Non-isothermal kinetic analysis of reversible ageing in asphalt cements. *Road Mater. Pavement Des.*, 18(4), 185–210.
18. Hesp S.A.M., Smith B.J., Hoare T.R., 2001. The effect of the filler particle size on the low and high temperature performance in asphalt mastic and concrete. *J. Assoc. Asphalt Pav. Tech.*, 70E, 1–19.
19. Liu Y., Su P., Li M., You Z., Zhao M., 2020. Review on evolution and evaluation of asphalt pavement structures and materials. *J. Traffic Transp. Eng.*, 7(5), 573–599.
20. Sun L., 2016. *Structural behavior of asphalt pavements: Integrated analysis and design of conventional and heavy duty asphalt pavement*. Butterworth-Heinemann.
21. Little D., Allen D., Bhasin A., 2018. *Modeling and design of flexible pavements*. Berlin: Springer.

22. Ren X., Ma J., Hesp S.A.M., 2023. Another look at the semi-circular bend test for the performance ranking of hot mix asphalt. *Constr. Build. Mater.*, 395, 132367.
23. Khabaz F., Khare R., 2018. Molecular simulations of asphalt rheology: Application of time–temperature superposition principle. *J. Rheol.*, 62(4), 941–954.
24. McCloskey K., Nivitha M.R., Ma J., Hesp S.A.M., Krishnan, J.M., 2023. Effects of temperature and age on stress relaxation in straight and modified asphalt binders from a northern Ontario pavement trial. *Road Mater. Pavement Des.*, 24(sup1), 336–351.
25. Iliuta S., Andriescu A., Hesp S.A.M., Tam K.K., 2004. Improved approach to low-temperature and fatigue fracture performance grading of asphalt cements. *Proc., Can. Tech. Asphalt Assoc.*, 123–158.
26. Khan A., Akentuna M., Pan P., Hesp S., 2020. Repeatability, reproducibility, and sensitivity assessments of thermal and fatigue cracking acceptance criteria for asphalt cement. *Constr. Build. Mater.*, 243, 117956.
27. Li Y., Hesp S.A., 2021. Enhanced Acceptance Specification of Asphalt Binder to Drive Sustainability in the Paving Industry. *Materials*, 14(22), 6828.
28. Ma J., Dean G., Nawarathna H., Hesp S., 2023. Development and validation of an accurate, precise and safe method for the acceptance testing of recovered asphalt binder. *Constr. Build. Mater.*, 409, 133960.
29. Petersen, J.C., Robertson, R.E., Branthaver, J.F., Harnsberger, P.M., Duvall, J.J., Kim, S.S., Anderson, D.A., Christensen, D.W., Bahia, H.U., Dongre, R., Antle, C.E., Sharma, M.G., *Binder Characterization and Evaluation; Volume 4: Test Methods, SHRP-A-370, National Research Council, Washington, D.C., 1994.*
30. ASTM D5, 2006. Standard Test Method for Penetration of Bituminous Materials. American Society for Testing and Materials.
31. Pumphrey M.E., 2003. Evaluation of performance graded asphalt binder equipment and testing protocol. West Virginia University.
32. McLeod N.W., 1978. Test data from three Ontario test roads after 15 years of service. *Proc., Can. Tech. Asphalt Assoc.*, 23, 534–610.
33. ASTM D2170, 2007. Standard Test Method for Kinematic Viscosity of Asphalts (Bitumens). American Society for Testing and Materials.
34. ASTM D4402, 2023. Standard Test Method for Viscosity Determination of Asphalt at Elevated Temperatures Using a Rotational Viscometer. American Society for Testing and Materials.
35. Gavin J., Dunn L., Juhasz M., 2003. Long Term Performance Monitoring of the Lamont Test Road. Paper presented at the Long-Life Pavements – Contributing to Canada’s Infrastructure Session of the 2003 Annual Conference of the Transportation Association of Canada St. John’s, Newfoundland and Labrador.
36. AASHTO R 320, 2023. Standard Specification for Performance-Graded Asphalt Binder. American Association of State Highway and Transportation Officials. Washington, D.C.
37. D'Angelo J., 2009. Current status of Superpave binder specification. *Road Mater. Pav. Des.*, 10, 13-24.
38. Mix design methods for asphalt concrete and other hot-mix types (No. 2). Asphalt Institute, 1997.
39. Bahia H., 1997. Applicability of Superpave to modified binders. *J. Transp. Res. Board*, 1586(1), 16–23.
40. Bahia H.U., Zhai H., Onnetti K., Kose S., 1999. Non-linear viscoelastic and fatigue properties of asphalt binders. *J. Assoc. Asphalt Paving Technol.* 68, 1–34.
41. Chen J.S., Tsai C.J., 1999. How good are linear viscoelastic properties of asphalt binder to predict

rutting and fatigue cracking? *J. Mater. Eng. Perform.* 8, 443–449.

42. D'Angelo J., Dongré R., 2002. Superpave binder specifications and their performance relationship to modified binders. *Proc., Can. Tech. Asphalt Assoc., Calgary, Alberta.*

43. Hesp S.A.M., Shurvell H.F., 2012. Waste engine oil residue in asphalt cement. *Proceedings, Seventh International Conference on Maintenance and Rehabilitation of Pavements and Technological Control, Auckland, New Zealand, 28–30.*

44. Hu M., Ma J., Sun D., Ling S., Lu T., Ni H., 2021. Understanding the aging depth gradient distribution of high viscosity modified asphalt. *ACS Sustain. Chem. Eng.*, 9(45), 15175–15189.

45. Hu M., Hofko B., Sun D., Mirwald J., Hofer K., Eberhardsteiner L., Lu T., 2023. Microevolution of Polymer–Bitumen Phase Interaction in High-Viscosity Modified Bitumen during the Aging of Reactive Oxygen Species. *ACS Sustain. Chem. Eng.*, 11, 8916–8930.

46. Ma J., Hu M., Sun D., Lu T., Sun G., Ling S., Xu L., 2021. Understanding the role of waste cooking oil residue during the preparation of rubber asphalt. *Resour. Conserv. Recycl.*, 167, 105235.

47. Ma J., Hu M., Lu T., Sun D., Hesp S.A.M., 2023. Thermo-reversible aging in biorejuvenated asphalt binder. *J. Clean. Prod.*, 383, 135404.

48. Zhang J., Ma J., Hesp S.A.M., 2024. Development of a simple and quantitative oil exudation test for asphalt binder. *Constr. Build. Mater.*, 415, 135003.

49. Bahia H.U., Hanson D.I., Zeng M., Zhai H., Khatri M.A., Anderson R.M., 2001. Characterization of modified asphalt binders in Superpave mix design (Project No. 9-10, FY 96).

50. Andriescu A., Hesp S.A.M., Youtcheff J.S., 2004. Essential and plastic works of ductile fracture in asphalt binders. *Transp. Res. Rec., J. Transp. Res. Board, No. 1875, 1–8.*

51. Andriescu A., Gibson N.H., Hesp S.A.M., Qi X., Youtcheff J.S., 2006. Validation of the essential work of fracture approach to fatigue grading of asphalt binders. *J. Assoc. Asphalt Pav. Tech.*, 75, 1016–1052.

52. Johnson C., Bahia H., Wen H., 2009. Practical application of viscoelastic continuum damage theory to asphalt binder fatigue characterization. *J. Assoc. Asphalt Pav. Tech.*, 78, 597–638.

53. Hajj R., Bhasin A., 2018. The search for a measure of fatigue cracking in asphalt binders—a review of different approaches. *Int. J. Pavement Eng.*, 19(3), 205–219.

54. Andriescu A., Iliuta S., Hesp S.A.M., Youtcheff J.S., 2004. Essential and plastic works of ductile fracture in asphalt binders and mixtures. *Proc., Can. Tech. Asphalt Assoc., Vol. 49, 93–122.*

55. Zofka A., Marasteanu M.O., 2007. Development of double edge notched tension (DENT) test for asphalt binders. *J. Test. Eval.*, 35(3), 259–265.

56. Paliukaitė M., Assuras M., Silva S., Ding H., Gotame Y., Nie Y., Ubaid I., Hesp S., 2017. Implementation of the double-edge-notched tension test for asphalt cement acceptance. *Transp. Dev. Econ.*, 3, 1–10.

57. Kim S.S., 2005. Direct measurement of asphalt binder cracking. *J. Mater. Civ. Eng.*, 17(6), 632–639.

58. Wagoner M.P., Buttlar W.G., Paulino G.H., 2005. Development of a single-edge-notched beam test for asphalt concrete mixtures. *J. Test. Eval.*, 33(6), 452.

59. Gibson N., Qi X., Shenoy A., Al-Khateeb G., Kutay M.E., Andriescu A., Stuart K., Youtcheff J., Harman T., 2012. Performance testing for Superpave and structural validation (No. FHWA-HRT-11-045). United States. Federal Highway Administration.

60. Ministry of Transportation of Ontario, 2015. Determination of Asphalt Cement's Resistance to Ductile Failure Using DENT, LS-299. Rev. 29, MTO Laboratory Testing Manual.
61. Auditor General of Ontario, 2016. Value for Money Audit, Ministry of Transportation—Road Infrastructure Construction Contract Awarding and Oversight, 2016 Annual Report from the Office of the Auditor General of Ontario.
62. AASHTO TP 113, 2015. Determination of asphalt binder's resistance to ductile failure using DENT test. American Association of State Highway and Transportation Officials. Washington, D.C.
63. Campbell S., Ding H., Hesp S.A.M., 2018. Double-edge-notched tension testing of asphalt mastics. *Constr. Build. Mater.*, 166, 87–95.
64. Ding H., Tetteh N., Hesp S.A.M., 2017. Preliminary experience with improved asphalt cement specifications in the City of Kingston, Ontario, Canada. *Constr. Build. Mater.*, 157, 467–475.
65. Ding H., Gyasi J., Hesp S.A.M., Marks P., Nie Y., Somuah M., Tabib S., Tetteh N., Ubaid I., 2018. Performance grading of extracted and recovered asphalt cements. *Constr. Build. Mater.*, 187, 996–1003.
66. AASHTO T 405, 2023. Determination of asphalt binder's resistance to ductile failure using double-edge-notched tension (DENT) test. American Association of State Highway and Transportation Officials. Washington, D.C.
67. Roy S.D., Hesp S.A.M., 2001. Fracture energy and critical crack tip opening displacement. *Proc., Can. Tech. Asphalt Assoc.*, 46, 187–214.
68. Hubbard P., Pritchard F., 1916. Effect of controllable variables upon the penetration test for asphalts and asphalt cements, *J. Agric. Res.*, 5 (17) 805–818.
69. Pendleton W.W., 1943. The penetrometer method for determining the flow properties of high viscosity fluids. *J. Appl. Phys.*, 14, 170–180.
70. Traxler R.N., Coombs C.E., 1936. The colloidal nature of asphalt as shown by its flow properties. *J. Phys. Chem.*, 40(9), 1133-1147.
71. Traxler R.N., Schweyer H.E, 1936. Increase in viscosity of asphalts with time. *Proc., ASTM*, 36, 544-551.
72. Traxler R., Coombs C., 1937. Development of internal structure in asphalts. *Proc., ASTM*, 37, 549-555.
73. Pechenyi B.G., Kuznetsov O.I., 1990. Formation of Equilibrium Structures in Bitumens. Translated from *Khimiya I Tekhnologiya Topliv I Masel*, 7, 32–34.
74. Bahia H.U., Anderson D.A., 1991. Isothermal low-temperature physical hardening of asphalt. *Proc., Int. Symp. Chem. Bitum.*, June 5-8, Rome, Italy, Vol. 1, pp. 114–147.
75. Bahia H.U., Anderson D.A., 1993. Glass transition behavior and physical hardening of asphalt binders (with discussion), *J. Assoc. Asphalt Pav. Tech.* 62, 93–129.
76. Basu A., Marasteanu M., Hesp S., 2003. Time-temperature superposition and physical hardening effects in low-temperature asphalt binder grading. *Transp. Res. Rec., J. Transp. Res. Board*, 1829(1), 1–7.
77. Ministry of Transportation of Ontario, 2015. Determination of Performance Grade of Physically Aged Asphalt Using EBBR Method, LS-308, Rev. 29, MTO Laboratory Testing Manual.
78. Iliuta S., Hesp S., Marasteanu M., Masliwec T., Tam K., 2004. Field validation study of low-temperature performance grading tests for asphalt binders. *Transp. Res. Rec., J. Transp. Res. Board.*, 1875(1), 14–21.79. Yee P., Aida B., Hesp S.A.M., Marks P., Tam K.K., 2006. Analysis of premature low-temperature cracking in three Ontario, Canada, pavements. *Transp. Res. Rec., J. Transp. Res. Board*, No. 1962, 44–51.

80. Hesp S.A.M., Subramani S., 2009. Another look at the bending beam rheometer for specification grading of asphalt cements. Proceedings, Sixth International Conference on Maintenance and Rehabilitation of Pavements and Technological Control, Torino, Italy, 1–10.
81. Erskine J., Hesp S.A.M., Kaveh F., 2012. Another look at accelerated aging of asphalt cements in the pressure aging vessel, June 13-15, Proc., Fifth Eurasphalt & Eurobitume Congress, Istanbul.
82. Akentuna M., Ding H., Khan A.N., Li Y., Hesp S.A.M., 2021. Improved performance grading of asphalt cement and hot mix asphalt in Ontario, Canada. *Int. J. Pav. Res. Technol.* 14, 267–275.
83. Li Y., Ding H., Nie Y., Hesp S.A.M., 2021. Effective control of flexible asphalt pavement cracking through quality assurance testing of extracted and recovered binders. *Constr. Build. Mater.*, 273, 121769.
84. Li Y., Hesp S.A.M., 2022. On the use of empirical phase angle limits for the grading of asphalt binder. *Constr. Build. Mater.*, 346, 128413.
85. Lill K., Kontson K., Khan A., Pan P., Hesp S.A.M., 2019. Comparison of physical and oxidative aging tendencies for Canadian and Northern European asphalt binders. Proc., Can. Tech. Asphalt Assoc., 24–28.
86. Coombs C.E., Traxler R.N., 1937. Rheological properties of asphalts IV. Observations concerning the anomalous flow characteristics of air-blown asphalts. *J. Appl. Phys.*, 8, 291–296.
87. AASHTO TP 122, 2016. Determination of Performance Grade of Physically Aged Asphalt Binder Using the Extended Bending Beam Rheometer (BBR) Method. American Association of State Highway and Transportation Officials. Washington, DC.
88. AASHTO T 406, 2023b. Determination of Performance Grade of Physically Aged Asphalt Binder Using the Extended Bending Beam Rheometer (BBR) Method. American Association of State Highway and Transportation Officials. Washington, D.C.
89. AASHTO R 28, 2012. Accelerated Aging of Asphalt Binder Using a Pressurized Aging Vessel (PAV). American Association of State Highway and Transportation Officials. Washington, D.C.
90. Hajek J.J., Phang W.A., Wrong G.A., Prakash, A., Stott, G.M., 1986. Pavement condition index (PCI) for flexible pavements. Report PAV-86-02. Ministry of Transportation, Downsview, Ontario, Canada.
91. Phang W.A., Chong G.J., 1981. Ontario flexible pavement distress assessment for use in pavement management. *Transp. Res. Rec., J. Transp. Res. Board*, 893, 51–59.
92. Mneina A., Smith J., 2022. Harmonization of pavement condition evaluation for enhanced pavement management: An Ontario case study. Transportation Association of Canada Conference and Exhibition.
93. Rubab S., Burke K., Wright L., Hesp S.A.M., Marks P., Raymond C., 2011. Effects of engine oil residues on asphalt cement quality. Proc., Can. Tech. Asphalt Assoc., 56, 1-12.
94. Wright L., Kanabar A., Moulton E., Rubab S., Hesp S.A.M., 2011. Oxidative aging of asphalt cements from an Ontario pavement trial. *Int. J. Pav. Res. Technol.*, 4(5) (2011).
95. Chan S., Bell H., Marks P., Lee S., 2018. Performance of Hot In-place Recycling the Kenora By-Pass. Proc., Can. Tech. Asphalt Assoc., 265–284.
96. Ma J., Nivitha M.R., Hesp S.A.M., Krishnan, J.M., 2023. Validation of empirical changes to asphalt specifications based on phase angle and relaxation properties using data from a northern Ontario, Canada pavement trial. *Constr. Build. Mater.*, 363, 129776.
97. Ding H., Zhang H., Liu H., Qiu Y., 2021. Thermoreversible aging in model asphalt binders. *Constr. Build. Mater.*, 303, 124355.